Analytical Evaluation of the Negative-Sequence Impedance Directional Elements in IBR-Rich Transmission Systems

Ghansham Meghwar
Electrical and Computer Engineering
University of Illinois Chicago
Chicago, United States
gmeghw2@uic.edu

Lina He
Electrical and Computer Engineering
University of Illinois Chicago
Chicago, United States
lhe@uic.edu

***Abstract*—The increasing penetration of Inverter-Based Resources (IBRs) fundamentally redefines grid fault characteristics, challenging legacy protection systems designed for synchronous generators. This paper presents a comparative analysis of the performance of a negative-sequence impedance directional element at various locations within a transmission network characterized by IBR integration. Using PSCAD/EMTDC simulations on a modified IEEE 39-bus system, the study evaluates the impact of an IEEE 2800-2022 compliant photovoltaic (PV) system and a non-compliant Type-IV wind farm (WF) on the relay's performance, benchmarking their response against that of a conventional synchronous generator (SG). The analysis will examine relay performance at the point of interconnection, remote-end buses, adjacent lines, and in parallel-infeed scenarios to provide a comprehensive understanding of the dependability and security challenges IBRs introduce to existing protection schemes.**

***Index Terms*—Directional Element, IEEE 2800-2022, Inverter-Based Resources (IBRs), Power System Protection, Protective Relaying.**

I. Introduction

Driven by environmental imperatives and declining generation costs, renewable energy sources (RESs) are rapidly transforming the traditional electrical grid into a power electronics-dominated system. This fundamental shift alters grid fault dynamics and presents a formidable challenge to the reliability of legacy protective relays [1]-[3]. According to the Solar Energy Industry Association (SEIA), the installed U.S. photovoltaic (PV) capacity is projected to more than double in the next five years, underscoring the need to address these challenges [4].

This paper is based upon work supported by the U.S. Department of Energy (DOE) Solar Energy Technologies Office (SETO) and Wind Energy Technologies Office (WETO) under the Solar and Wind Grid Services and Reliability Demonstration Funding Program, Award Number: DE-EE0010656. This research was conducted at the University of Illinois Chicago.

The core issue lies in the disparity between traditional protection philosophies and the behavior of modern Inverter-Based Resources (IBRs). Protection methods for transmission networks, including differential, distance, and directional schemes, were developed based on the fault characteristics of synchronous generators (SGs), which supply large, predictable fault currents due to their physical inertia [1],[5],[6]. In contrast, IBRs exhibit unique fault behaviors, including limited fault current amplitude, controlled current phase, and variable sequence impedance, all of which are dictated by their power-electronic control strategies rather than physical laws [7],[8]. Collectively, these characteristics fundamentally undermine the operating principles of legacy relays, which may consequently fail to detect or correctly respond to a fault [9], [10].

Initially, the impact of RESs was mitigated by disconnecting them during faults. However, with their continuously increasing penetration, this practice now poses a threat to overall system stability [1], [11]. Consequently, modern grid codes, such as the German Grid Code and IEEE 2800-2022, mandate that IBRs must ride through faults (FRT) [12],[13]. This shift presents a fundamental challenge to legacy protection schemes, particularly during unbalanced faults. Many of these schemes, including negative-sequence overcurrent (50Q/51Q) and directional (67Q) relays, depend entirely on the presence of negative-sequence currents to operate correctly [14]. Yet, traditional IBRs using coupled sequence control (CSC) are often designed to suppress these exact currents, creating a critical vulnerability in the protection scheme [15]. This is not merely a theoretical concern; it can lead to a complete failure to trip, as was demonstrated in a 2022 event in the Dominion Energy territory where a fault was not accurately identified due to the lack of negative-sequence current from an IBR facility [16]. In response, newer grid codes may require or allow IBRs to inject negative-sequence current via decoupled sequence control (DSC), which in turn creates new, complex interactions with protection systems that must be thoroughly understood [15].

979-8-3315-8138-1

The literature widely documents that the unique fault characteristics of IBRs pose significant challenges to conventional protection schemes. Foundational studies establish that IBRs with traditional controls contribute a significantly lower magnitude of negative-sequence current during unbalanced faults compared to SGs, and the phase angle relationship between negative-sequence voltage and current is changed [8],[14],[17]. This behavior directly impacts negative-sequence-based relays, causing instantaneous overcurrent (50Q) elements to fail to pick up and directional overcurrent (67Q) elements to incorrectly determine the fault direction. To address these shortcomings, researchers have validated the effectiveness of modern grid codes, such as the German VDE-AR-N 4120, which mandate negative-sequence current injection to restore correct relay operation [14],[17].

However, two critical gaps persist in the existing body of research. First, there is a lack of analysis focused specifically on the impact of the latest generation of IBRs compliant with the comprehensive IEEE 2800-2022 standard. While older grid code solutions have been studied, the influence of modern, decoupled sequence controls as specified in this new standard remains a crucial area for analysis. Second, much of the research is localized, focusing on the impact at the immediate IBR tie-line [18] or utilizing smaller, custom test systems [8]. A comprehensive understanding of how the fault response of a modern IBR propagates and affects protection relays at various buses within a large, interconnected transmission network is missing.

To address these critical research gaps, this paper presents a comparative analysis of protection system performance at various network locations. The primary contribution is an evaluation of the system-wide impact of a modern, IEEE 2800-2022 compliant PV system with decoupled sequence controls and a traditional Type-IV wind farm, directly benchmarking their response against a conventional SG. To move beyond localized studies, these diverse generation sources are modeled within the standard IEEE 39-bus transmission system. Using this system model, the performance of the negative-sequence impedance directional element is analyzed at multiple locations. This methodology enables a broader understanding of how modern IBR controls impact protection, security, and dependability, extending far beyond their immediate point of interconnection.

The remainder of this paper is organized as follows. Section II details the generation source models and the principles of protection elements. Section III describes the test system and simulation setup. Section IV presents and analyzes the simulation results from various case studies, and Section V concludes the paper with a summary of the key findings.

II. IBR Control Architectures and Protection Principles

A. Generation Source Models

The analysis in this paper compares the fault response of two distinct IBRs against the benchmark performance of a conventional SG. The SG's response is governed by its inherent physical properties, providing a predictable, high-magnitude fault current with both positive and negative-sequence components, the baseline around which legacy protection is designed. In contrast, the IBRs' responses are dictated by their control strategies, as detailed below.

1) Control Structure of the Non-Compliant Type-IV Wind Farm: The non-compliant WF is modeled as a Type-IV wind turbine, with its Grid-Side Converter (GSC) managed by a standard vector control strategy, as illustrated in Fig. 1 [19]. This strategy operates in the positive-sequence synchronous reference frame to manage both active and reactive power; however, its conventional design lacks specific responses to negative-sequence components during unbalanced faults.

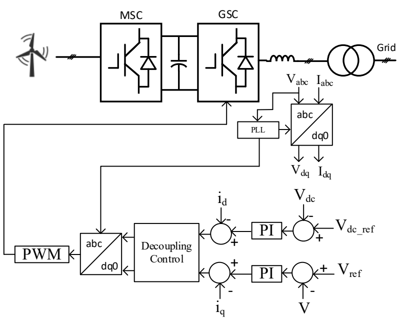

Fig. 1. Standard vector control strategy for the GSC of a Type-IV wind farm

2) Control Structure of the Compliant PV System: The IEEE 2800-2022 compliant PV system is managed by an advanced vector control strategy designed to provide grid support during both balanced and unbalanced conditions [20]. The control architecture is based on a dual-sequence framework, which explicitly decomposes the grid currents and voltages into their positive and negative sequence components, as shown in Fig. 2.

The outer control loops regulate active and reactive power according to their setpoints, while also incorporating FRT logic as mandated by the standard. Aligning with IEEE 2800-2022 Clause 7, the control logic injects negative-sequence reactive current proportional to the negative-sequence voltage deviation, thereby ensuring the requisite grid support during unbalanced faults. This is achieved through dedicated inner current controllers and a positive/negative sequence decoupling network, ensuring a precise and stable response. A current-limiting function is also included to ensure the inverter's operational limits are never exceeded, providing a predictable fault characteristic.

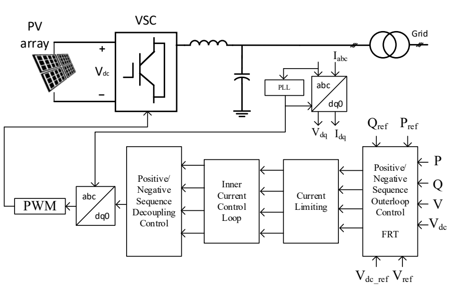

Fig. 2. Control architecture of the IEEE 2800-2022 compliant PV system

979-8-3315-8138-1

B. *Negative-Sequence Impedance Directional Element*

The protection element under study is the negative-sequence impedance directional element, based on the logic presented in [21]. This element is designed to detect all types of unbalanced faults, including phase-to-phase and phase-to-ground faults, by analyzing negative-sequence quantities. The core of its logic is based on calculating the negative-sequence quantities to determine the direction of a fault. The operation of the element is governed by five key settings.

The primary directional decision is made by the forward and reverse negative-sequence impedance thresholds, Z2F and Z2R, respectively. A measured impedance (Z_2) that is less than the Z2F setting is classified as a forward fault, while a measured impedance greater than the Z2R setting is considered a reverse fault. To ensure a clear distinction, the Z2R setting is always more positive than the Z2F setting.

To ensure that a fault condition of sufficient magnitude exists, the directional logic is supervised by forward and reverse negative-sequence overcurrent elements, 50QF and 50QR, respectively. These elements act as fault detectors and operate based on three times the negative-sequence current ($3I_2$). For a forward fault to be declared, the magnitude of $3I_2$ must exceed the 50QF setting, and for a reverse fault, it must exceed the 50QR setting.

Finally, a positive-sequence current restraint factor (a2) provides additional security to prevent incorrect operation during balanced (three-phase) fault conditions. Line asymmetries can cause small negative-sequence quantities to appear during balanced faults. The a2 element prevents the relay from tripping in such cases by requiring the negative-sequence current (I_2) to be a significant fraction of the positive-sequence current (I_1) before the element is allowed to operate.

III. System Modeling and Simulation Setup

A. *Test System: Modified IEEE 39-Bus System*

For this study, a modified version of the IEEE 39-bus system is used as the test bed, with the analysis performed using simulations in PSCAD/EMTDC. The single-line diagram of this test bed is depicted in Fig. 3. This system is a well-established benchmark for power system stability and protection studies, making it an ideal choice for this study. The primary modification involves connecting IBRs and an SG at Bus 36. This centralized integration strategy was explicitly selected to isolate the fundamental impact of IBR control dynamics on protection logic, establishing a clear performance baseline without the confounding interaction effects of distributed multi-infeed IBRs.

B. *Component Modeling in PSCAD*

The power system model shown in Fig. 3 was developed in PSCAD/EMTDC, with all generation sources (SG, Type-IV WF, and Compliant PV) implemented using identical nominal power ratings. Furthermore, modern IBRs introduce non-linear control dynamics that make analytical impedance loci derivations infeasible for large networks. Consequently, this study relies on high-fidelity time-domain simulations to empirically characterize relay performance. Similarly, control parameters were held constant to representative industry values to isolate protection challenges inherent to the control architecture, distinct from secondary variations introduced by specific parameter tuning.

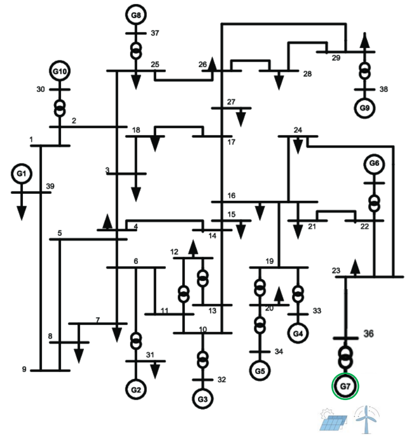

Fig. 3. Single-line diagram of the modified IEEE 39-bus test system

The pickup thresholds and other settings for the modeled relays were not generic; instead, they were systematically determined based on the relay's specific location within the transmission network. The settings were calculated using the electrical characteristics of the corresponding protected line, with parameters such as line impedance being sourced directly from the PSCAD transmission line models. Relay logic was implemented in PSCAD, using standard library components and Fast Fourier Transform (FFT) blocks to extract the fundamental and sequence components from voltage and current waveforms. This approach ensures that the relay settings are appropriately tailored to their designated protection zone.

IV. Simulation Results and Discussion

This section analyzes the directional element's performance across the three generation scenarios. In all subsequent figures, Red denotes the SG (baseline), Blue the non-compliant WF, and Black the compliant PV.

A. *Case 1: Performance at the IBR Point of Interconnection*

The initial case establishes the core protection challenge by simulating a forward Phase A to ground (AG) fault on line 36-23, with the relay located at the IBR interconnection bus 36. The results for this case are presented in Fig. 4. In the baseline scenario, the SG provides a robust, high-magnitude negative-sequence current (I_2), causing all relay elements to operate instantaneously for a correct, high-speed trip. This represents the benchmark for dependable performance. When the SG is replaced by the non-compliant WF, the relay's performance is critically compromised. The WF fails to inject significant I_2, leaving the fault detector (50QF) unasserted. This lack of response effectively blinds the relay, leading to a complete failure to trip. The compliant PV system presents a more nuanced challenge. It actively injects I_2, which allows the directional (Z2F) and supervisory (a2) elements to operate correctly. However, this current magnitude is insufficient to meet the legacy forward fault detector setting, thereby

979-8-3315-8138-1

preventing a trip. This case demonstrates the two primary failure modes for relays at an IBR's point of interconnection: complete blinding due to a non-compliant IBR's lack of response, and a sensitivity challenge where a compliant IBR's response is directionally correct but insufficient for legacy settings.

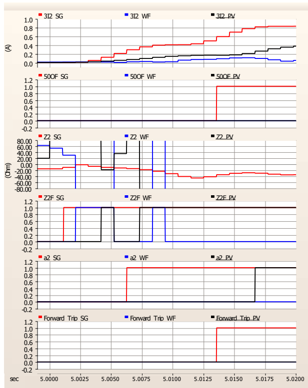

Fig. 4. Relay performance at Bus 36 towards Bus 23 for a forward AG fault on Line 36-23

B. *Case 2: Performance at the Remote-End Bus*

The analysis next considers a relay at the remote end of the line (bus 23), looking back towards the IBR at bus 36. As shown in Fig. 5(a) for a forward fault on line 23-36, the relay operates correctly and instantaneously in all three generation scenarios. Due to the low impedance path from the relay to strong conventional sources behind it (such as generator G6 at bus 22), the I_2 measured by the relay is dominated by these sources, rendering the behavior of the remote-end source at bus 36 negligible.

To assess the impact of directionality and fault impedance, a reverse fault was then simulated at bus 23, with the corresponding results displayed in Fig. 5(b). While the SG provided an almost immediate trip, the non-compliant WF failed to operate. In contrast, the compliant PV successfully initiated a trip, albeit with a noticeable delay. This delay was directly attributable to the slow ramp-up of the PV's injected I_2, which postponed the operation of the 50QR element. However, when this reverse fault was moved 50% down the line, the added fault impedance reduced the PV's current contribution to a level below the 50QR threshold, causing the relay to fail to detect the fault. This demonstrates that while a remote relay's forward reach remains unaffected, its ability to detect reverse faults fed by an IBR is highly sensitive to the relay's settings and the location of the fault. This creates a "shrinking zone of protection" for reverse faults, which could leave line sections unprotected.

C. *Case 3: Performance on an Adjacent Line*

This section evaluates relay performance on a line (23-24) adjacent to the line connected to the IBR (23-36), with the relay at bus 23 looking towards bus 24. The waveforms in Fig. 6(a) demonstrate that for a solid forward fault, the relay trips are almost instantaneously and identically in all three cases. In this scenario, the negative-sequence current (I_2) is sourced almost exclusively from the strong grid at bus 22. Because the

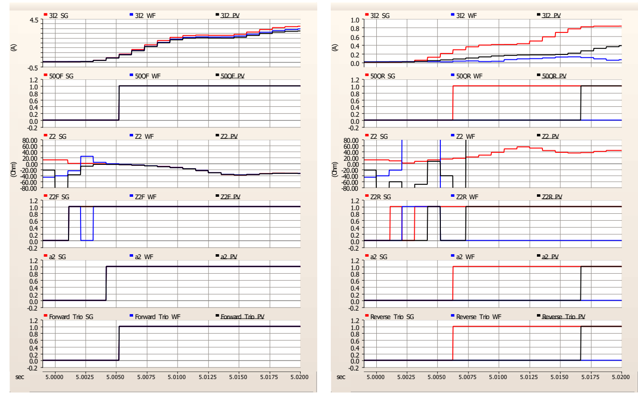

(a) (b)

Fig. 5. Relay performance at Bus 23 towards Bus 36 (a) for a forward AG fault on Line 23-36 (b) for a reverse fault at Bus 23

IBR at bus 36 is located on a separate, non-faulted line, it has no significant impact on the relay's measurement. This secure operation was also observed for reverse faults on this line.

However, in this case, when the forward fault resistance is increased to 20 Ω, a performance degradation is observed. While the SG still provides an instantaneous trip, both the compliant PV and non-compliant WF exhibit a delayed trip. The high fault impedance induces a slower, ramp-like current injection from the inverters, which in turn delays the operation of the 50QF fault detector. The impact of IBRs is therefore localized during solid faults but can cause tripping delays on adjacent lines during high-impedance faults.

D. *Case 4: Impact of Parallel IBR Infeed*

The final case examines a relay on line 23-22 looking towards the strong grid, where the relay measures the combined I_2 from the grid (via line 23-24) and the generator at bus 36 (via line 23-36). In the baseline scenario, the strong infeed from the SG combines with the grid contribution to produce a very high I_2, resulting in an instantaneous trip, as illustrated in Fig. 6(b). When SG is replaced by IBRs, its weaker current contribution substantially reduces the total I_2 measured by the relay. The lower total I_2, combined with the slower inverter response, causes a delay in the pickup of the 50QF fault detector, which in turn delays the final trip. This case study illustrates that IBRs can have a systemic impact; by weakening the I_2 contribution from a parallel path, they can reduce the total I_2 seen by a relay and slow its fault-clearing time, potentially affecting grid stability and protection coordination.

Although the presented analysis focuses on representative single-line-to-ground (SLG) faults at key locations, the underlying study evaluated a broader range of unbalanced fault types (including phase-to-phase) and additional relay locations (e.g., Buses 22 and 24). The protection element's response remained qualitatively consistent across these extensive simulations, confirming that the reported cases effectively capture the core performance challenges. Crucially,

979-8-3315-8138-1

the observed phenomena, specifically the negative-sequence deficiency, are intrinsic to the IBR control architecture rather than the specific network topology. Consequently, these fundamental failure modes (blinding and sensitivity loss) are expected to persist across varying fault conditions and multi-infeed scenarios, validating the generalizability of these findings.

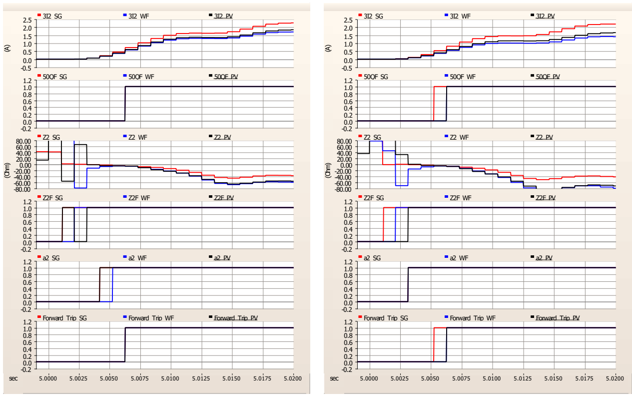

(a) (b)

Fig. 6. Relay performance at (a) Bus 23 towards Bus 24 for a forward AG fault on Line 23-24, (b) Bus 23 towards Bus 22 for a forward fault on Line 23-22

V. Conclusion

This paper presents a comparative analysis of the performance of a negative-sequence directional element in a transmission system with significant IBR penetration, benchmarking a non-compliant Type-IV wind farm and an IEEE 2800-2022 compliant PV system against a conventional synchronous generator. The results show that a non-compliant IBR can blind a relay element by failing to produce sufficient negative-sequence current. Although the compliant PV system provides a directionally correct signal, its current-limited response creates a critical sensitivity issue, preventing relays at the point of interconnection from tripping under legacy settings.

The study further demonstrates that the impact of IBRs extends beyond their connection point, causing significant tripping delays for reverse faults, shrinking protection zones, and slowing down relays on adjacent and parallel lines, especially during high-impedance faults. Ultimately, this research confirms that even modern, grid-code-compliant IBRs pose significant dependability and security challenges. To address these limitations, future research should prioritize adaptive protection schemes that dynamically adjust sensitivity thresholds and evaluate their robustness in complex, multi-infeed IBR scenarios.

References

[1] Z. Yang, H. Wang, W. Liao, C. L. Bak, and Z. Chen, "Protection challenges and solutions for AC systems with renewable energy sources: a review," *Protection and Control of Modern Power Systems*, vol. 10, pp. 18-39, Jan. 2025.

[2] M. Nagpal, M. Jensen, and M. Higginson, "Protection challenges and practices for interconnecting inverter-based resources to utility transmission systems," IEEE Power & Energy Society, Tech. Rep., pp. 1–65, 2020.

[3] G. Meghwar, S. Yu, and L. He, "An enhanced fault detection strategy based on the transient voltage in multi-terminal HVDC grid," in *Proc. 2024 IEEE Power & Energy Society General Meeting (PESGM)*, pp. 1-5.

[4] Wood Mackenzie, "US solar market insight Q3 2023," 2023. [Online]. Available: https://www.woodmac.com/industry/power-and-renewables/us-solar-market-insight/

[5] N. M. Varghese and M. K. Jena, "Reconceptualizing the transmission line protection from the perspective of IBR-dominated grid," *IEEE Access*, vol. 12, pp. 195065-195075, 2024.

[6] A. A. Memon, A. Kumar, G. Sham, and U. Yasir, "Automated protection of power transformers at distribution grid connected to green energy sources," in *Proc. 2018 IEEE Canadian Conference on Electrical & Computer Engineering (CCECE)*, pp. 1-4.

[7] C. Chao et al., "Collaborative solution of distance protection and dual current control for outgoing lines of inverter-based resources during line-to-line faults," *IEEE Trans. Smart Grid*, vol. 15, pp. 3782-3794, Jul. 2024.

[8] A. Haddadi, I. Kocar, and E. Farantatos, "Impact of inverter-based resources on protection schemes based on negative sequence components," EPRI, Palo Alto, CA, Tech. Rep. 36.1, 2019.

[9] K. W. Jones et al.,"Impact of inverter-based generation on bulk power system dynamics and short-circuit performance," IEEE Power & Energy Society, Task Force on Short-Circuit and System Performance Impact of Inverter-Based Generation, Tech. Rep. PES-TR68, Jul. 2018.

[10] G. Meghwar, D. Weicheng, M. Bawazeer, and J. Xu, "Reciprocating connection of dual active bridge DC/DC converter with PV integration," in *Proc. 2020 5th International Conference on Power and Renewable Energy (ICPRE),* pp. 566-571.

[11] M. Bawazeer, D. Weicheng, G. Meghwar, and J. Xu, "Reciprocating bus in FREEDM system with solar farm integration," in *Proc. 2020 5th International Conference on Power and Renewable Energy (ICPRE)*, pp. 27-32.

[12] Technical Requirements for the Connection and Operation of Customer Installations to the Extra High Voltage Network (TCR Extra High Voltage), VDE-AR-N 4130, Nov. 2018.

[13] IEEE Standard for Interconnection and Interoperability of Inverter-Based Resources (IBRs) Interconnecting With Associated Transmission Electric Power Systems, IEEE Std. 2800-2022, Apr. 2022.

[14] A. Haddadi, M. Zhao, I. Kocar, U. Karaagac, K. W. Chan, and E. Farantatos, "Impact of inverter-based resources on negative sequence quantities-based protection elements," *IEEE Trans. Power Delivery*, vol. 36, pp. 289-298, Feb. 2021.

[15] T. Kauffmann et al., "Short-circuit model for type-IV wind turbine generators with decoupled sequence control," *IEEE Trans. Power Delivery*, vol. 34, pp. 1998–2007, Oct. 2019.

[16] T. Nguyen, B. Alexander, and P. Doss, "Investigating a transmission line misoperation caused by IBR penetration," unpublished.

[17] A. Haddadi et al., "Negative sequence quantities-based protection under inverter-based resources: Challenges and impact of the German grid code," *Electric Power Systems Research*, vol. 188, p. 106573, 2020.

[18] R. Guttromson, "Impact of inverter-based resource (IBR) negative sequence current injection on transmission system protection," Sandia National Laboratories, Albuquerque, NM, Tech. Rep. SAND2020-7324C, Jul. 2020.

[19] S. Heier, *Grid Integration of Wind Energy Conversion Systems. Chichester*, UK: Wiley, 1998.

[20] R. Mahmud, A. Hoke, J. Keen, and J. Cale, "Developing IEEE Std 2800-compliant algorithms for transmission-connected inverter-based resources," in *Proc. 2024 IEEE 52nd Photovoltaic Specialist Conference (PVSC)*, pp. 1170-1175.

[21] B. Fleming, "Negative-sequence impedance directional element," in Proc. 10th Annual ProTest User Group Meeting, pp. 1–11, Feb. 1998.

979-8-3315-8138-1